

Minniti D. & Zijlstra A. 1996 *ApJ*, **467**, L13.  
 Lee M.G., Aparicio A., Tikonov N., Byun Y.-I. & Kim E. 1999 *AJ*, **118**, 853.  
 Saha A., Sandage A., Labhardt L., Tammann G.A., Macchetto F.D. & Panagia N. 1996 *ApJ*, **466**, 65.  
 Skillman E.D., Kennicutt R.C. & Hodge P. 1989 *ApJ*, **347**, 875.  
 Smecker-Hane T.A., Stetson P.B., Hesser J.E. & Lehnert M.D. 1994 *AJ*, **108**, 507.

Steidel C.C., Adelberger K.L., Giavalisco M., Dickinson M. & Pettini M. 1999, *ApJ*, **519**, 1.  
 Tolstoy E. & Saha A. 1996, *ApJ*, **462**, 672.  
 Tolstoy E., Gallagher J.S., Cole A.A., Hoessel J., Saha A., Dohm-Palmer R.C., Skillman E.D., Mateo M. & Hurley-Keller D. 1998, *AJ*, **116**, 1244.  
 Tolstoy E. 1998, XVIIIth Moriond Astrophysics Meeting: *Dwarf Galaxies and*

*Cosmology*, eds. T.X. Thuan et al., in press (astro-ph/9807154).  
 Tolstoy E. 1999, IAU Symposium 192, *The Stellar Content of Local Group Galaxies*, eds. Whitelock & Cannon, p. 218.  
 Tosi M., Focardi P., Greggio L. & Marconi G. 1989, *The Messenger*, **57**, 57.  
 Tosi M., Greggio L., Marconi G. & Focardi P. 1991, *AJ*, **102**, 951.  
 Whiting A.B., Hau G.K.T. & Irwin M. 1999, *AJ*, **118**, 2767.

## FIRES at the VLT: the Faint InfraRed Extragalactic Survey

M. FRANX<sup>1</sup>, A. MOORWOOD<sup>2</sup>, H.-W. RIX<sup>3</sup>, K. KUIJKEN<sup>4</sup>, H. RÖTTGERING<sup>1</sup>,  
P. VAN DER WERF<sup>1</sup>, P. VAN DOKKUM<sup>1</sup>, I. LABBE<sup>1</sup>, G. RUDNICK<sup>3</sup>

<sup>1</sup>Leiden Observatory, <sup>2</sup>ESO, <sup>3</sup>MPIA, <sup>4</sup>University of Groningen

One of the unique capabilities of the VLT is the near-infrared imaging mode of ISAAC. The wide field of view, detector stability, and image quality that ISAAC can provide are currently unparalleled at other observatories.

In order to take advantage of this window of opportunity, we have proposed a non-proprietary, deep imaging survey. The survey consists of very deep exposures in the  $J_s$ , H and  $K_s$  bands of the Hubble Deep Field South (Williams et al. 2000), and somewhat shallower imaging on a wider field in the cluster MS1054-03 at  $z = 0.83$  (Gioia and Luppino 1994, van Dokkum et al. 1999, 2000). The survey is aimed at the study of distant galaxies in both fields, although many other applications will be possible. The same fields are observed at other wavelengths by several other groups. The full complement of data will range from the radio to the X-ray. The fields were selected based on their superb optical imaging from the Hubble Space Telescope. Both fields will be observed for a total of 96 hours, split evenly between  $J_s$ , H and  $K_s$ . In the field of MS1054-03, this integration time will be divided between four pointings to cover the full Hubble Space Telescope mosaic of images (van Dokkum et al. 2000). For the Hubble Deep Field South, one single pointing will cover the WFPC image. The expected depth of the images is a  $K_s$  magnitude of 24.4 (26.3) in the HDF South, and a  $K_s$  magnitude of 23.7 (25.6) in MS1054-03; these are  $3\sigma$  limits in Johnson and AB magnitudes, respectively. The OPC has been very generous and has allocated the full requested time to this survey.

The first data on the Hubble Deep Field South were obtained at the end of 1999. Even the first quarter of the total integration provided  $K_s$ -band data of unprecedented image depth and quality for the HDFs. A colour image is

shown in Figure 1, which is a combination of the HST I band data, and  $J_s$  and  $K_s$  ISAAC data. The variations among the infrared colours of galaxies are striking, and several very red galaxies are immediately apparent in the image.

Some of these galaxies are absent, or very faint in the extremely deep I band data from the Hubble Space Telescope.

Some examples of distant galaxies are shown in Figure 2. The morphologies of the very red galaxies span a

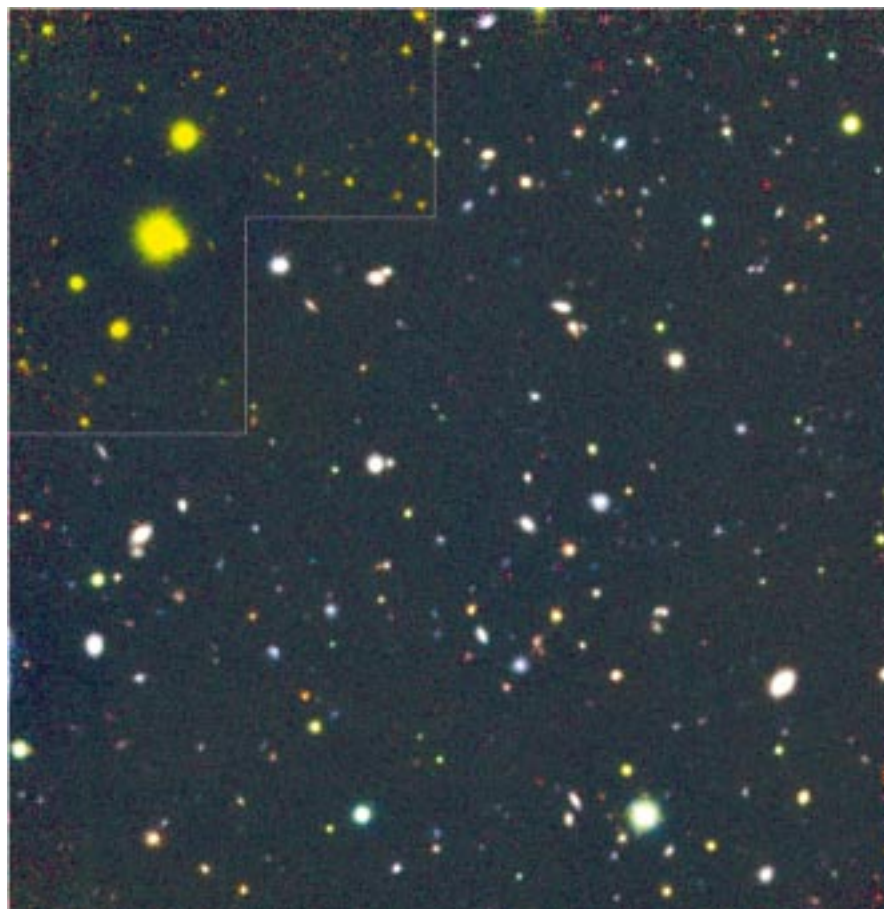


Figure 1. A colour image of the Hubble Deep Field South, observed with the Hubble Space Telescope, and ISAAC on the VLT. The colour image is constructed from the I band images from HST, and the  $J_s$  and  $K_s$  images taken with ISAAC. The outline indicates the size and shape of the WFPC2 field, and the galaxy colours outside of that are yellow-green because of the absence of I band data in the image. The great variety of galaxy colours is striking. These differences are often caused by redshift: at higher redshifts, the Balmer break and 4000 Angstrom break will move in or beyond the bandpass of the I band filter. Some very red galaxies can be identified, these have very low I and  $J_s$  fluxes.

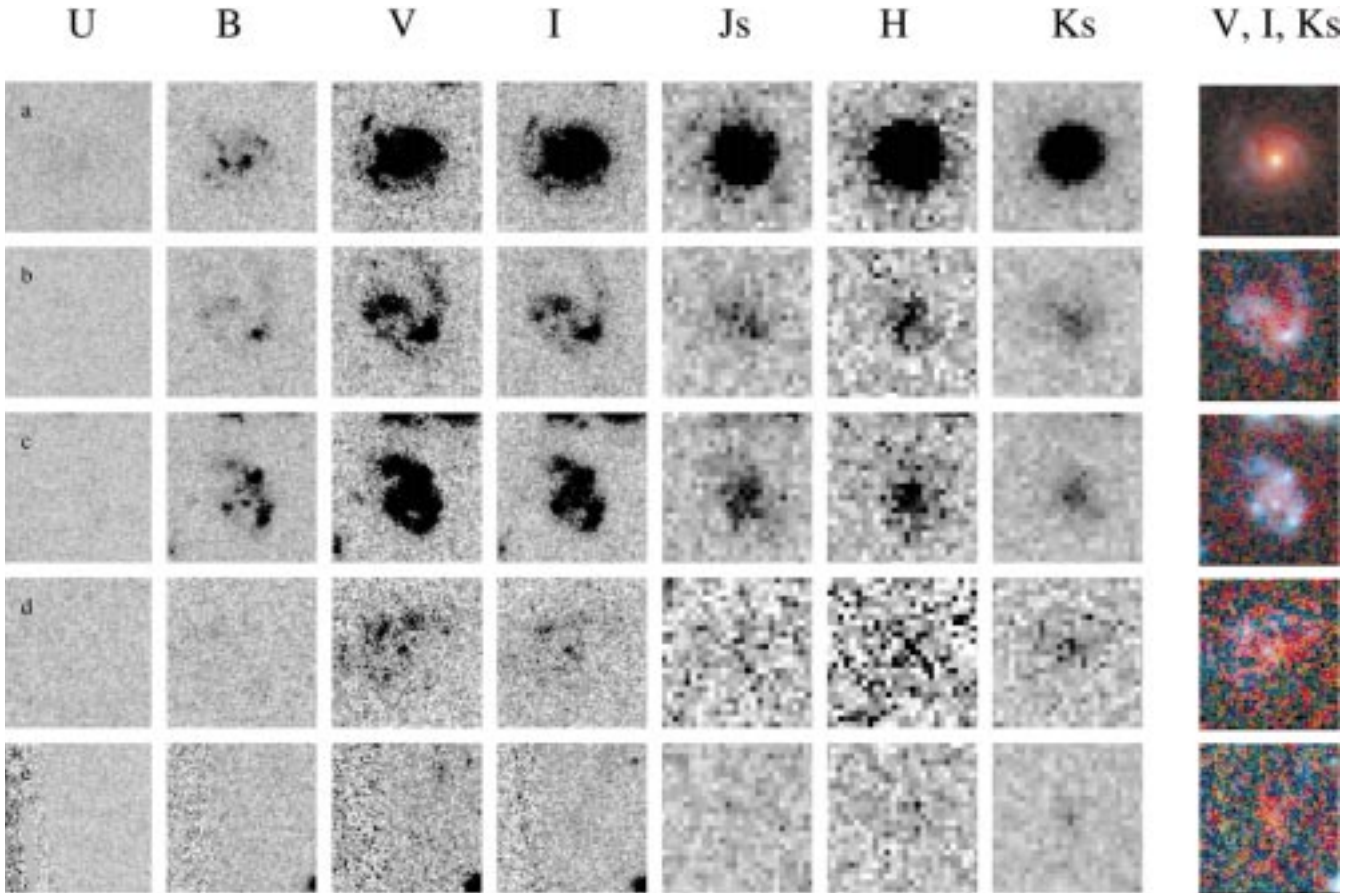


Figure 2. A close-up of several high-redshift galaxies in the Hubble Deep Field South. The individual panels show the images of the galaxies in the optical from HST (U, B, V, I), and in the infrared from the VLT ( $J_s$ , H,  $K_s$ ). The differences in morphology are quite striking. Thanks to the good image quality of the VLT data, many of the galaxies are resolved in the infrared. The large galaxy in panel d is similar to spiral galaxies in the nearby universe. It is likely at a redshift above 2. The galaxy in panel e has not been identified as a galaxy from the HST-WFPC data, whereas it is bright in the infrared. Such very red galaxies can contribute substantially to the stellar mass density at high redshift.

wide range: some are compact at all wavelengths, others are compact in the infrared, but much more extended in the optical wavelengths. The very red colours of these galaxies are likely caused by the redshifted Balmer or 4000-Angstrom breaks or by dust. The spectral energy distributions of three of the galaxies are shown in Figure 3. The redshift of the galaxy in Figure 3a is expected to be above 1.6, whereas the others are expected to be above 2 based on their spectral energy distribution.

Some of the morphologies are quite remarkable. The very large galaxy in Figure 2d is an example. It is very extended in the I band, which most likely corresponds to the rest-frame UV. The HST images show spiral structure, similar to that of spiral galaxies nearby. The  $K_s$  band image show a centrally concentrated component, which is likely the bulge of the galaxy. This galaxy is therefore possibly the progenitor of a large-disk galaxy at low redshift. If this is confirmed with deeper data, it would be in conflict with theories of disk formation which predict generally small disks at high redshift. Another striking example is shown in Figure 2e. This galaxy has extremely weak I band emission, and was not included in the source list of galaxies for the HDF South (Williams et al. 2000), but we

note that it is close to the edge between WF and PC. The galaxy in Figure 2c is red in the I- $J_s$ , but very blue in the optical colours. It is a regular Ly-Break galaxy, with a remarkable difference in morphology between the IR and optical. The Ly-break would predict the Balmer break to occur further to the red (redward of  $J_s$ ). Further study is required to see whether dust or other factors may play a role.

The first results of the survey are very promising. When the survey is completed, it will be unique in terms of depth and coverage. The data can be used for many purposes: the study of J drop-out objects, which are possibly the highest redshift galaxies (e.g., Dickinson et al. 1999); the study of the rest-frame optical properties of Ly-break galaxies, the determination of photometric redshifts of a large sample of galaxies, especially for galaxies with redshifts between 1 and 3; the weak lensing signal in the Hubble Deep Field South and MS1054-03, aided by accurate photometric redshifts; the faint end of the luminosity function at lower redshifts, both for the field and MS 1054-03, etc.

One of the interesting applications is the selection of distant galaxies purely based on their observed infrared fluxes. As we have shown in Figures 2 and 3, some galaxies are very red in their  $J_s$ -

$K_s$  and/or  $J_s$ -H colours. These galaxies are so faint in the optical, that they will generally not be in samples selected by the Ly-break technique (Steidel et al. 1996). Nevertheless, their contribution to the total (rest-frame) optical luminosity density at high redshift can be quite substantial. Given the fact that their mass-to-light ratio is also expected to be higher than that of Ly-break galaxies, their contribution to the stellar mass density at high redshift could be significant. Analysis of this aspect is in progress.

The reduced data of the survey will be made available to the public. We expect a first release of the preliminary HDF South data later this year. The data reduction is relatively complex due to the large number of frames taken in jitter mode, some of which were affected by scattered moonlight. For the most accurate astrometry and combination with other images, it is also necessary to correct for a small amount of field distortion.

We have currently written our own reduction routines based on the IRAF "dimsum" package. The observations on the cluster field MS1054-03 are expected to be done soon, but they have not yet started.

Updates on the programme can be found at our web site <http://www.strw.leidenuniv.nl/~franx/fires>.

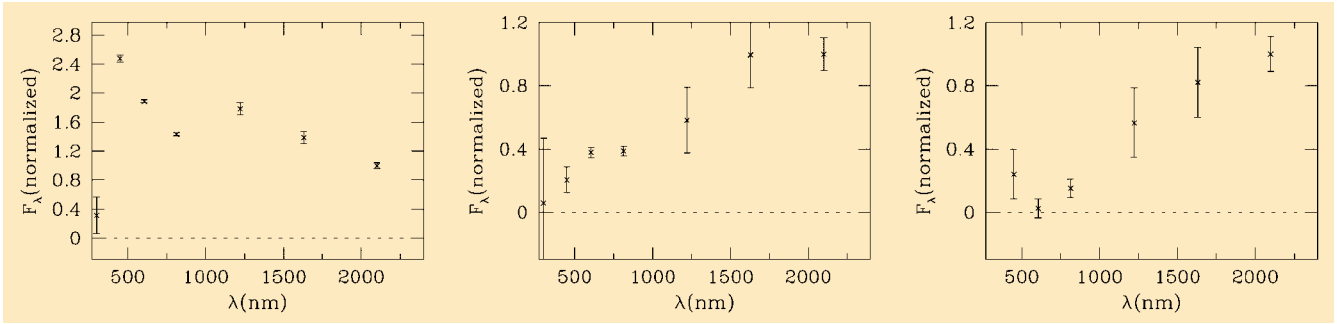


Figure 3: The normalised spectral energy distribution of 3 galaxies. From left to right we show a regular Ly-break galaxy (Fig. 2c), the “spiral” galaxy (Fig. 2d), and the very red galaxy from Figure 2e. The red continuum feature of the last two galaxies can be due to the Balmer/4000 Angstrom break or due to dust. Only one of these would be selected by the regular Ly-break selection technique, as the others are too faint in the optical (rest-frame UV).

### Acknowledgement

It is a pleasure to thank the staff at ESO who contributed to the construction and operation of the VLT and ISAAC. This project has only been possible because of their enormous efforts.

### References

Dickinson, M., et al, 1999, preprint, astro-ph/9908083.  
 Gioia, I., and Luppino, G. A., 1994, *ApJS*, **94**, 583.  
 van Dokkum, P. G., Franx, M., Fabricant, D., Kelson, D., Illingworth, G. D., 1999, *ApJL*, **520**, L95.

van Dokkum, P. G., Franx, M., Fabricant, D., Kelson, D., Illingworth, G. D., 2000, submitted to *ApJ*.  
 Steidel, C. C., Giavalisco, M., Pettini, M., Dickinson, M., Adelberger, K. L., 1996, *ApJL*, **462**, L17.  
 Williams, R. E., et al, 2000, in preparation.

# Optical Observations of Pulsars: the ESO Contribution

R.P. MIGNANI<sup>1</sup>, P.A. CARAVEO<sup>2</sup> and G.F. BIGNAMI<sup>3</sup>

<sup>1</sup>ST-ECF, [rmignani@eso.org](mailto:rmignani@eso.org); <sup>2</sup>IFC-CNR, [pat@ifctr.mi.cnr.it](mailto:pat@ifctr.mi.cnr.it); <sup>3</sup>ASI [bignami@asi.it](mailto:bignami@asi.it)

### Introduction

Our knowledge of the optical emission properties of neutron stars has been remarkably improved by the results obtained during the last 15 years. At the beginning of the 80s, only two of the about 500 isolated neutron stars at that time detected as radio pulsars had been identified also at optical wavelengths. These were the two young (2000–10,000 years) optical pulsars in the Crab (Cocke et al. 1969), the first and for about 10 years the only one, and Vela (Wallace 1977) supernova remnants. Soon after the identification of the Crab, a model to explain the optical emission of young pulsars was developed by Pacini (1971) in terms of synchrotron radiation emitted by charged particles injected in the pulsar’s magnetosphere. According to this model, the optical luminosity of a pulsar is predicted to scale proportionally to  $B^4P^{-10}$ , where B and P are its magnetic field at the light cylinder and its period, respectively. This relation, known as the “Pacini’s Law”, proved correct for both the Crab and the Vela pulsars and was thereon assumed as a reference.

The panorama of neutron stars’ optical astronomy changed rapidly when few more pulsars started to be identified (or discovered) in the X-ray data of the EINSTEIN satellite (see Seward and Wang 1988 for a review) and a possible X-ray counterpart for the enig-

matic gamma-rays source Geminga, not yet recognised as an X/gamma-ray pulsar, was proposed. This triggered the search for their optical counterparts,

and ESO telescopes gave to the European astronomers the chance to boost a virtually new field of investigation (see Table 1 for a summary of the

	1985	90	95	00
CRAB		NTT*	2.2m*	VLT VLT
B1509–58		NTT*	3.6m* NTT* NTT*	VLT
B0540–69		3.6m 3.6m NTT* 3.6m	NTT → HST	VLT
VELA	3.6m* 2.2m 3.6m*	NTT*	3.6m 3.6m NTT* → HST	VLT
B0656+14		3.6m* NTT*	→ HST	
GEMINGA	3.6m*	NTT*	NTT* NTT* → HST NTT	
B1055–52	3.6m*		NTT* → HST	

IMAGING SPECTROSCOPY  
TIMING POLARIMETRY

Table 1: Summary of (published) ESO observations of the pulsars with an optical counterpart. For each pulsar the observing epochs and the telescopes are listed. Observations performed by the authors are marked by an asterisk. The observing modes are specified by the colour code. Arrows indicate HST follow-ups. The results are summarised in Table 2 and described in the text.